14-3-3 Proteins Associate with Phosphorylated Simple Epithelial Keratins during Cell Cycle Progression and Act as a Solubility Cofactor

Jian Liao and M. Bishr Omary

VA Palo Alto Health Care System, 154 J, Palo Alto, California 94304; and the Digestive Disease Center, Stanford University School of Medicine, Palo Alto, California 94305

Abstract. 14-3-3 is a ubiquitous protein family that interacts with several signal transduction kinases. We show that 14-3-3 proteins associate with keratin intermediate filament polypeptides 8 and 18 (K8/18) that are expressed in simple-type epithelia. The association is stoichiometrically significant (≥ one 14-3-3 molecule/keratin tetramer), occurs preferentially with K18, and is phosphorylation- and cell cycle–dependent in that it occurs during S/G2/M phases of the cell cycle when keratins become hyperphosphorylated. Binding of phospho-K8/18 to 14-3-3 can be reconstituted in vitro using recombinant 14-3-3 or using total cellular cytosol. Phosphatase treatment results in dissociation of 14-3-3, and dephosphorylation of phospho-K8/18 prevents reconstitution of the binding. Three cellular keratin subpopulations were analyzed that showed parallel gradients of keratin phosphorylation and 14-3-3 binding. Incubation of 14-3-3 with keratins during or after in vitro filament assembly results in sequestering of additional soluble keratin, only in cases when the keratins were hyperphosphorylated. Our results demonstrate a stoichiometrically significant cell cycle– and phosphorylation-regulated binding of 14-3-3 proteins to K18 and in vitro evidence of a simple epithelial keratin sequestering role for 14-3-3 proteins.

Of the three major cytoskeletal (CSK)[1] protein groups in higher eukaryotes, intermediate filament (IF) proteins are the least understood in functional terms as compared with microfilaments and microtubules (for review see Steinert and Roop, 1988; Klymkowsky et al., 1989; Skalli and Goldman, 1991; Fuchs and Weber, 1994). Several unique features distinguish IF proteins from the other two major CSK protein families. First, IF proteins make up a large and tissue-specific group of cytoplasmic and nuclear proteins that include keratins in epithelial cells, neurofilaments in neuronal cells, vimentin in mesenchymal cells, desmin in muscle cells, and lamins in nuclei. Of the IF protein subgroups, keratins are the largest with >20 mucosal or "soft" keratin (K1–K20) gene products, which exclude the "hard" keratins that are found in epidermal appendages such as hair and nails. Similar to other IF protein subgroups, keratins are expressed in a tissue and cell preferential manner (Moll et al., 1982, 1990, 1993; Eckert, 1988; Stasiak et al., 1989; Calnek and Quaroni, 1993). For example, simple-type glandular epithelia, as in the intestine, liver, and pancreas, express predominantly keratin polypeptides 8 and 18 (K8/18) with variable levels of K19 and K20 depending on the cell type and differentiation state. Similarly, keratinocytes express K1/10 and/or K5/14 depending on their maturation level within the epidermis. Second, mutations in eleven different keratin proteins that include K5, K14, K1, K10, K9, K2e (for review see Fuchs et al., 1994; McLean and Lane, 1995), K16, K17 (McLean et al., 1995), K6a (Bowden et al., 1995), K4 (Rugg et al., 1995), K13 (Richard et al., 1995), and in neurofilament-H (Figlewicz et al., 1994) result in human skin, oral, and neuromuscular diseases. Third, IF proteins are considered nearly insoluble, although in the case of human K8/18, ~5% of the keratin pool is soluble (Chou et al., 1993).

The dynamic nature of IF proteins and their tissue-specific expression suggest that they are likely to play important cellular functions although the evidence to date for a number of potential functions is limited. Examples of proposed functions include a role in signal transduction (e.g., Baribault et al., 1989; Omary et al., 1992; Busso et al., 1994), cholesterol transport (for review see Evans, 1994), and gene regulation (for review see Traub and Shoeman, 1994). Based on the well-understood regulation of many

Address reprint requests to Jian Liao and other correspondence to M. Bishr Omary, VA Palo Alto Health Care System, 3801 Miranda Avenue, 154 J, Palo Alto, CA 94304.

1. *Abbreviations used in this paper*: C, cytosolic; CSK, cytoskeletal; Emp, Empigen BB; G cell, G0/G1 cell cycle stage enriched; hsp, heat shock protein; IF, intermediate filament; M cell, G2/M phases enriched; OA, okadaic acid; PAP, potato acid phosphatase; PKC, protein kinase C; r, recombinant; S cell, S phase enriched; 2-D, two-dimensional.

biological systems, the most likely candidates for the regulation of IF protein dynamics and presumed function(s) include posttranslational modifications and associated regulatory proteins. In the case of K8/18, phosphorylation (Oshima, 1982; Celis et al., 1983) occurs on serine residues and is a dynamic modification that increases in a reversible manner during the S and G2/M phases of the cell cycle (Chou and Omary, 1994; Liao et al., 1995*a*). K8/18 phosphorylation increases under conditions of cell stress including heat and virus infection (Liao et al., 1995*b*). Mutation of a major phosphorylation site of human K18 interferes with the ability of K8/18 filaments to reorganize upon G2/M arrest in transfected cells (Ku and Omary, 1994), and in vitro phosphorylation of purified K8/18 interferes with filament assembly (Yano et al., 1991). With regard to K8/18 associated proteins, several have been identified by coimmunoprecipitation, which include a protein kinase C (PKC) ε–related kinase (Omary et al., 1992), a membrane-associated 85-kD protein (Chou et al., 1994), and two members of the heat shock protein (hsp) 70 family (Liao et al., 1995*c*).

The 14-3-3 protein family, which was first identified in rabbit brain and named based on its migration in starch gels (Moore and Perez, 1967), is increasingly invoked in carrying out important roles in signal transduction and progression through the cell cycle (for review see Aitken, 1995; Burbelo and Hall, 1995). For example, several kinases including Raf (Freed et al., 1994; Fu et al., 1994; Irie et al., 1994), PKC (Robinson et al., 1994), c-Bcr and Bcr-Abl (Reuther et al., 1994), and PI3-kinase (Bonnefoy-Bérard et al., 1995) bind to 14-3-3, and as a consequence may have their kinase activity altered by this binding depending on the experimental conditions used. In the cases studied, 14-3-3 binding to other associated proteins appears to require their phosphorylation as demonstrated for Raf and Bcr (Michaud et al., 1995) and tryptophan hydroxylase (Furukawa et al., 1993). In this report, we show that 14-3-3 associates with K8/18 intermediate filament proteins in a phosphorylation- and cell cycle–regulated and –reversible manner. The association of 14-3-3 with K8/18 involves the soluble cytosolic, and nonionic detergent-solubilized K8/18 pools that become hyperphosphorylated during the S and G2/M phases of the cell cycle and does not involve the remaining relatively insoluble and substantially less phosphorylated cytoskeletal K8/18 pool. Furthermore, 14-3-3 acts as a solubility cofactor for K8/18, and its binding to phospho-K8/18 is abolished upon dephosphorylation of the keratins. Our studies suggest a model whereby two abundant epithelial cellular protein families regulate each other in a cell cycle– and phosphorylation-dependent manner.

Materials and Methods

Cells and Reagents

All human cell lines (HT29, T84 and CaCO2 [colon] HeLa [cervix]; Molt4 [T cell]; MCF7 [breast]) and MDCK (canine kidney) were obtained from the American Type Culture Collection (Rockville, MD). Human colonic biopsies were obtained from patients undergoing colonoscopies for medically indicated reasons under a protocol approved by the Human Subjects Committee at Stanford University. mAbs used were: L2A1 (Chou and Omary, 1993), CK5, and 8.13 (Sigma Chemical Co., St. Louis, MO), which recognize different epitopes of K18 (L2A1, CK5) or K8 and K18 (8.13); and 4.62 which recognize K19 (Sigma Chemical Co.). Rabbit antibody 8592 (Ku et al., 1995) was also used to immunoprecipitate K8 and K18 individually. Recombinant (r) bovine brain 14-3-3ζ isoform and rabbit anti-14-3-3 ζ, γ, η were from Upstate Biotechnology Inc. (UBI) (Lake Placid, NY). Carrier-free $^{32}PO_4$ was purchased from DuPont-New England Nuclear (Wilmington, DE). Other reagents used were: potato acid phosphatase (PAP) and aphidicolin (Sigma Chemical Co.), okadaic acid (OA) (LC Services, Woburn, MA), and soybean trypsin inhibitor (Worthington Biochemical Corp., Freehold, NJ).

Treatment with Okadaic Acid (OA), Heat Stress, and Cell Synchronization

Asynchronously growing confluent cells (mostly G0/G1 cell cycle stage enriched [G cells]) were treated with OA (1 μg/ml, 2 h) followed by harvesting. For heat stress, cells at ~50% confluency were incubated at 42°C for 24 h (Liao et al., 1995*b*). Cell synchronization was carried out by arresting cells at G1/S using the DNA polymerase-α inhibitor aphidicolin (5 μg/ml, 24 h) followed by washing off the drug and incubating with fresh media for 5–6 h (S phase enriched [S cells]), or 10–12 h (G2/M phases enriched [M cells]). Cell cycle analysis was carried out after fixing cells with 70% ethanol and then staining with propidium iodide (Chou and Omary, 1993).

Isolation and Analysis of Keratin Fractions

Keratins were isolated by immunoprecipitation from three cellular fractions. The cytosolic fraction was obtained after disrupting cells by nitrogen cavitation (150 psi, 5 min, 4°C) in PBS containing 10 mM EDTA, followed by centrifugation (16,000 g, 30 min, 4°C) and collecting the supernatant (C fraction). A 1,000× stock solution of protease inhibitors and okadaic acid was then used to obtain a final concentration equivalent to buffer A (PBS, 10 mM EDTA, 0.1 mM PMSF, 10 μM pepstatin, 10 μM leupeptin, 25 μg/ml aprotinin, 0.5 μg/ml OA) (see below). Similar results were obtained if centrifugation was done at 100,000 *g* for 90 min (not shown). The pellet was then solubilized with 1% NP-40 in buffer A (30 min, 4°C) followed by centrifugation (16,000 *g*, 15 min, 4°C) and collecting the NP-40 fraction. The pellet was then solubilized with 1% Empigen BB (Emp) in buffer A (Lowthert et al., 1995) (30 min, 4°C). After repelleting, the Emp-soluble supernatant was collected (cytoskeletal fraction). In some cases, the residual Emp-insoluble pellet was solubilized in 50 mM Tris-HCl, pH 7.4, 2 mM EDTA/9.5 M urea or in sample buffer. Alternatively, cells were solubilized directly with 1% NP-40 in buffer A. Immunoprecipitation was then done directly or after adjusting the solution fractions so that they all contained 1% NP-40 and 1% Emp, as described, except that incubation with antibody was for 6 h (Lowthert et al., 1995). SDS-PAGE (Laemmli, 1970), isoelectric focusing, immunoblotting, potato acid phosphatase treatment (Liao et al., 1995*b*,*c*), and tryptic phosphopeptide mapping (Boyle et al., 1991) were as described. In some cases, the two-dimensional gels were transferred to polyvinylidene difluoride membranes followed by Coomassie staining and then autoradiography if appropriate. Metabolic labeling with $^{32}PO_4$ (125 μCi/ml, 5 h) was done in RPMI 1640 medium containing 100 μM phosphate and 10% dialyzed FCS.

Identification of p29, 30, and 33 Proteins as 14-3-3η, ζ, and ε, Respectively

The p29, 30, and 33 proteins were isolated by coimmunoprecipitation with K8/18, from NP-40–solubilized S or G2/M phase cells, followed by separation using preparative SDS-PAGE gels. Individual bands were cut from the gel after brief staining with Coomassie blue followed by digestion with Lys C. Peptides released from the gel strips were separated by HPLC followed by microsequencing of prominent peaks. Three peptides were sequenced from p29 with sequences VFYL, DSTLIMQLL, and NLLSVAYK, which are conserved sequences of 14-3-3 proteins, and based on the apparent M_r of p29, are likely to correspond to human 14-3-3η residues 121–124, 218–226, and 43–50, respectively (Ichimura-Ohshima et al., 1992). Two peptides were sequenced from p30 digests with sequences GIVDQSQQAYQEAFEI and TAFDEAIAELDTLSEESYK, which correspond to residues 140–155 and 194–212 of sheep 14-3-3ζ, respectively (Roseboom et al., 1994). For p33, one peptide was sequenced that afforded the sequence YLAEFATGNDRK that corresponds to residues 131–142 of human 14-3-3ε (Conklin et al., 1995). All sequenced peptides showed 100% homology to the indicated regions (not shown).

Keratin Filament Assembly

K8/18 were purified by immunoprecipitation from NP-40–solubilized HT29 G or M cells. The residual pellet from the NP-40–solubilized M cells was then solubilized with 1% Emp followed by immunoprecipitation of K8/18. Nearly 40 (G cell) and 20 (M cell) 100-mm dishes were used to isolate the NP-40 fractions, respectively. Endogenously associated 14-3-3 was released by incubation of the immunoprecipitates with 1% Emp/PBS. Purified keratins were then released from the antibody by adding 9.5 M urea (no detectable antibody is released since it is covalently coupled to the agarose beads). Filament assembly was initiated by dialyzing 150 μl of the keratin urea solution (150 μg/ml), in the absence or presence of r14-3-3ζ or soybean trypsin inhibitor (40 μg/ml), against 50 mM Tris-HCl, 2 mM EDTA, pH 7.5, for 36 h (4°C) with one buffer change. Alternatively, K8/18 (150 μg/ml) was first dialyzed alone to allow filament assembly, followed by the addition of r14-3-3ζ or soybean trypsin inhibitor (62.5 μg/ml) and then gentle mechanical rotation (24 h, 4°C). The soluble and pellet fractions were separated by ultracentrifugation (68,000 *g*, 30 min, 4°C). Equivalent aliquots were analyzed by SDS-PAGE. Negative staining was done as described (Liao et al., 1995*c*).

Reconstitution of 14-3-3 Binding to K8/18

r14-3-3ζ, Molt4 NP-40 lysate, or HT29 cell cytosol were added to immunoprecipitates of K8/18. HT29 cell cytosol was obtained from G cells, as described above, followed by immunodepletion of K8/18 by three rounds of immunoprecipitation (immunodepletion was verified by SDS-PAGE analysis of the immunoprecipitates; not shown). Molt4 cells ($1.5\text{-}3 \times 10^7$) were solubilized in 1.5 ml of 1% NP-40 in buffer A (30 min, 4°C) followed by pelleting to collect the supernatant. K8/18 immunoprecipitates were then incubated with 1 ml of Molt4 lysate or HT29 cell cytosol, or with 0.2 ml of PBS containing 1 μg of r14-3-3ζ (30 min, 22°C). After washing three times with 1% NP-40 in PBS, samples were analyzed by SDS-PAGE.

Alternatively, K8 and K18 were individually purified from the cytosolic fraction of M cells by immunoprecipitation of K8/18, preparative SDS-PAGE, and then cutting out the K8 or K18 bands separately after visualization by copper staining. K8 and K18 were electroeluted followed by extraction of SDS, solubilization of the keratins in 9 M urea, and then dialysis against 1% NP-40 in PBS/2 mM EDTA to allow renaturation. Nonsolubilized material (~20% of total) was removed by high speed centrifugation, and purified solubilized K8 or K18 was then incubated with r14-3-3 followed by immunoprecipitation using anti-K8/18 antibody 8592.

Measurement of Stoichiometry of K8/18 and 14-3-3 Association

Serial dilutions of K8/18 standards (purified using FPLC from a high salt extract of HT29 cells) (Liao et al., 1995*b*) and r14-3-3ζ were used side by side on the same SDS-PAGE gel with K8/18 immunoprecipitates obtained from the cytosolic and NP-40 fraction of G and M cells. The relative levels of K8/18 and 14-3-3 isoforms were determined using densitometric scanning of Coomassie stained–destained gels with an enhanced laser densitometer (Ultrascan XL; LKB Instruments, Inc., Gaithersberg, MD). The protein content of soluble K8/18 and 14-3-3ζ in relation to the total cellular protein pool was determined by quantitative immunoblotting using 10 μg of total cell lysate (solubilized in 2% SDS-containing buffer) or analysis sample (e.g., cytosolic fraction). Using this method, the estimated total cellular keratin and soluble fraction gave very similar results to those obtained by Coomassie staining as described previously (Chou et al., 1993). Quantitation of the immunoblots and the two-dimensional gels was done using densitometric scanning.

Results

Characterization of 14-3-3 Association with K8/18/19

We used coimmunoprecipitation from the human colonic epithelial cell line HT29 to ask if any proteins associate with phosphorylated forms of K8/18/19. To enhance the sensitivity of identifying putative-associated proteins, hyperphosphorylation of K8/18/19 was achieved by incubating cultured cells in the presence of the phosphatase inhibitor OA. As shown in Fig. 1 *A*, immunoprecipitation of K8/18/19 from cells treated with OA and then solubilized with the nonionic detergent NP-40 resulted in coimmunoisolation of three species with apparent migration on SDS-PAGE of ~29, 30, and 33 kD (p29, 30, and 33). Depending on gel conditions, the p29 and 30 can sometimes be better resolved (e.g., Fig. 2 *A*, lanes *c–f*). These three species were absent from the K8/18 immunoprecipitate if cells were not treated with okadaic acid (Fig. 1 *A*, lane *b*) and did not bind to a nonspecific Ig control (Fig. 1 *A*, lane *a*). This suggests that hyperphosphorylation of the keratins and/or p29, 30, and 33 was needed for the observed interaction. The visibility of p29, 30, and 33 (Fig. 1, *A* and *B*) after Coomassie staining indicates that they are abundant species. The p29, 30, and 33 were identified as members of the 14-3-3 family η, ζ, and ϵ isoforms, respectively, after micro-sequencing of several peptides that were generated by Lys C digestion of the individual coimmunoprecipitated proteins (see Materials and Methods).

The association of 14-3-3 with K8/18/19 was abolished when cells were solubilized with the zwitterionic detergent Emp (Fig.1 *B*, lane *c*), and can be reconstituted after incubating with cytosol from Molt4 cells that do not express keratins but do express significant levels of 14-3-3 proteins (Fig. 1 *B*, lane *d*). Association of 14-3-3 with hyperphosphorylated K8/18/19 was also confirmed using two other monoclonal anti-K8/18 antibodies that recognize different epitopes than that recognized by mAb L2A1 (not shown). The interaction of 14-3-3 with phospho-K8/18/19 was also noted in several other cell lines that express K8/18 (T84, CaCO2, HeLa, MDCK, and MCF7 cells) and in normal human colonic biopsies after culturing the cells or the biopsy explants in the presence of OA (1 μg/ml for 2 h), but not in the absence of OA (not shown).

The identity of 14-3-3 as a phospho-K8/18/19–associated protein was further confirmed in two other ways. First, the association can be reconstituted using K8/18/19 immunoprecipitates, obtained from cells cultured at 42°C (which results in hyperphosphorylation of K8/18/19) (Liao et al., 1995*b*) or cells treated with OA and r14-3-3ζ (Fig. 1 *D*). Second, immunoblotting of K8/18 immunoprecipitates with anti-14-3-3ζ showed reactivity with p30 (14-3-3ζ) which comigrates with r14-3-3ζ (Fig. 1 *C*). The K8/18/19 immunoprecipitates were obtained from cells treated with OA and then solubilized with NP-40 to maintain endogenous 14-3-3 association (Fig. 1 *C*, lane *b*), or from OA-treated cells that were solubilized with Emp to release endogenous keratin-associated 14-3-3 and then incubated with Molt4 cell cytosol or K8/18/19-depleted HT29 cell cytosol (Fig. 1 *C*, lanes *c* and *d*). The Molt4 and HT29 cell cytosols were from cells not treated with OA. Taken together, this indicates that the reconstitution of keratin–14-3-3 association can occur using a variety of 14-3-3 sources and that phosphorylation of 14-3-3 is not required for binding to hyperphosphorylated K8/18/19.

Keratin Association with 14-3-3 Is Phosphorylation and Cell Cycle Regulated, Is Independent of hsp70 Binding, and Involves Binding to Phospho-K18

The binding of 14-3-3 to phospho-K8/18/19 prompted us to examine if similar binding can be demonstrated during the S and G2/M phases of the cell cycle, which are phases that

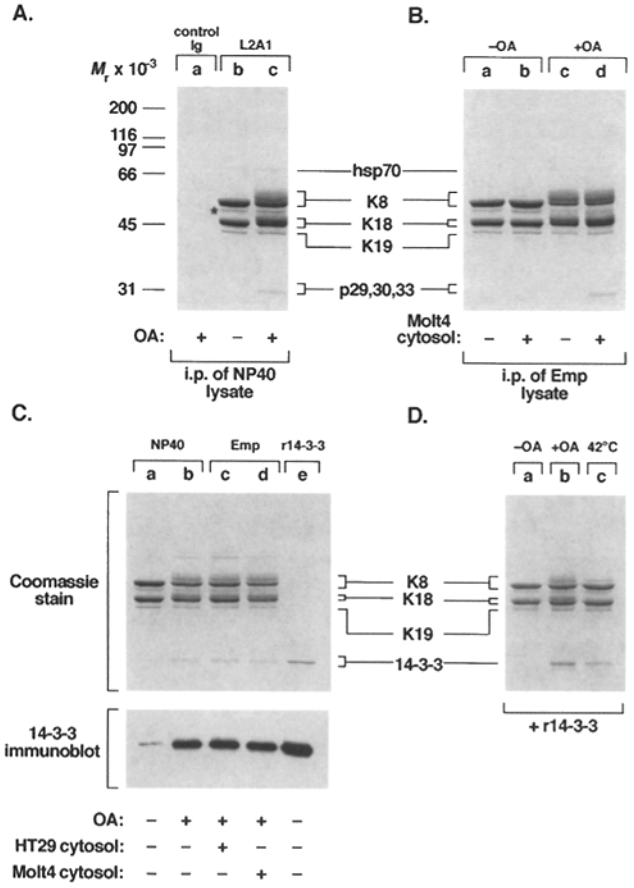

Figure 1. Characterization of 14-3-3 association with K8/18/19. (*A*) HT29 cells were cultured in the presence or absence of OA (1 μg/ml) for 2 h. Cells were then solubilized with 1% NP-40 in buffer A followed by immunoprecipitation using mAb L2A1 (which immunoprecipitates the keratins as noncovalent heteropolymers) or nonspecific control Ig conjugated to agarose. The band between K8 and K18 (*asterisk*) is variably seen with K8/18/19 immunoprecipitates and corresponds to K20 and/or partially degraded K8. (*B*) HT29 cells were cultured in the presence or absence of OA (1 μg/ml, 2 h) and then solubilized with 1% Emp in buffer A followed by immunoprecipitation of K8/18/19. Immunoprecipitates were incubated with a cytosolic fraction obtained from non-OA–treated human Molt4 cells (15 min, 22°C), washed four times with 0.5% NP-40 in buffer A and then analyzed by SDS-PAGE. (*C*) Immunoprecipitates of K8/18/19 were obtained from HT29 cells (with or without OA preincubation) followed by solubilization with 1% NP-40 or 1% Emp. Immunoprecipitates were incubated in the presence or absence of a cytosolic fraction obtained from HT29 (K8/18/19 immunodepleted) or Molt4 cells (15 min, 22°C) followed by washing off nonbound material. Equivalent portions of the washed immunoprecipitates were analyzed on two gels using SDS-PAGE followed by Coomassie staining of one gel (shown) and transfer of the second gel to a membrane for immunoblotting with anti–14-3-3ζ antibody. r14-3-3 (0.5 μg) was also analyzed on the same gel (lane *e*). (*D*) Immunoprecipitates of K8/18/19 were obtained from Emp-solubilized cells that were grown at 37°C in the presence or absence of OA, or from cells that were grown at 42°C (24 h). The immunoprecipitates were incubated with r14-3-3 for 15 min followed by washing, SDS-PAGE analysis, and Coomassie staining.

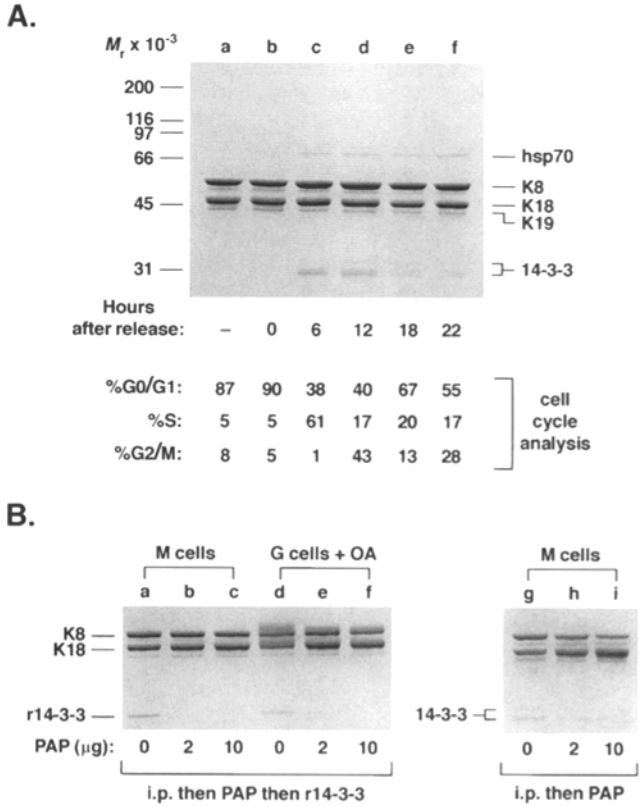

Figure 2. Association of 14-3-3 with K8/18/19 during the cell cycle and its regulation by phosphorylation. (*A*) Near confluent dishes of asynchronously growing HT29 cells (lane *a*) were blocked at G1/S using aphidicolin (lane *b*). Cells were then split and cultured in the absence of aphidicolin for the indicated times (lanes *c–f*). For each time point, cells from one dish were solubilized with 1% NP-40 followed by immunoprecipitation with mAb L2A1, and cells from a duplicate dish (identical to immunoprecipitation time points) were used for cell cycle analysis. (*B*) Immunoprecipitates of K8/18/19 were obtained from NP-40–solubilized OA-treated (1 μg/ml, 2 h) near confluent HT29 cells, which are primarily G cells, or from M cells as in *A*. The indicated immunoprecipitates were then incubated with PAP (lanes *g–i*) or 1% Emp in PBS to release bound 14-3-3 proteins, followed by dephosphorylation using PAP and incubation with r14-3-3 (lanes *a–f*).

are associated with hyperphosphorylation of K8/18 (Chou and Omary, 1994; Liao et al., 1995*a*). For this, cells were blocked at G1/S using aphidicolin, a DNA polymerase-α inhibitor, followed by release of the block to enrich for cells at the S and G2/M phases of the cell cycle. As shown in Fig. 2 *A*, significant association of 14-3-3 with K8/18/19 is noted during the S and G2/M phases of the cell cycle (lanes *c* and *d*), which decreases as cells exit G2/M and enter G1 (lane *e*), and then begins to increase again with increasing fraction of G2/M cells (lane *f*). This lends support to the findings in Fig. 1 and suggests that the K8/18/19 association with 14-3-3 is dependent on keratin phosphorylation. In addition, it indicates that the keratin–14-3-3 association occurs in a regulated manner during the cell cycle. The importance of keratin phosphorylation was further tested by treating K8/18/19 immunoprecipitates, obtained from mitotically enriched (M) cells, with PAP, which results in dissociation of the complex (Fig. 2 *B*, lanes *g–i*).

Similarly, reconstitution of K8/18/19 (isolated from M cells or OA-treated G cells) binding to r14-3-3 is prevented by phosphatase treatment (Fig. 2 *B*, lanes *a–f*).

Since the keratin–14-3-3 complex also contains hsp70, we asked if hsp70 is necessary for binding of 14-3-3 to K8/18/19. This was done by the addition of MgATP or MgGTP to K8/18/19 immunoprecipitates, which results in release of the coimmunoprecipitated hsp70 (Liao et al., 1995*c*). As shown in Fig. 3 *A*, addition of MgATP or MgGTP to K8/18/19 immunoprecipitates results in release of hsp70 but does not affect the keratin–14-3-3 binding (lanes *a–c*). Furthermore, MgATP-induced pre-release of hsp70 from a phosphokeratin–hsp70 complex, which was isolated from NP-40–solubilized OA-treated cells followed by the addition of Emp (to release bound 14-3-3), does not interfere with the reconstituted binding of r14-3-3 to phospho-K8/18/19 (Fig. 3 *A*, lanes *d* and *e*). This indicates that hsp70 and 14-3-3 binding to K8/18/19 is not interdependent.

We then asked which glandular keratin(s) play an important role in binding to 14-3-3. As shown in Fig. 3 *B*, preferential immunoprecipitation of K8/19 is not associated with 14-3-3 binding (lane *c*), whereas 14-3-3 does bind to the remaining K8/18 in the absence of K19 (lane *b*). This indicates that 14-3-3 proteins bind to K18 and/or to K8/18 and that not all keratins are involved in this binding. K18 was identified as the keratin of the K8/18/19 mix that binds to 14-3-3 by reconstitution of r14-3-3 binding with individually purified phospho-K8 or phospho-K18 (Fig. 3 *C*). It appears that a "native-like" K18 is needed for association with 14-3-3 since boiling of K8/18 immunoprecipitates decreases the efficiency of association, and binding cannot be reproduced in an overlay assay using K8/18/19 that was separated by SDS-PAGE (not shown).

Several Keratin Cellular Compartments Can Be Isolated that Manifest Parallel Keratin Phosphorylation and 14-3-3 Binding Gradients

To assess the relationship between keratin phosphorylation and its solubility and binding to 14-3-3, we analyzed cytosolic, NP-40–solubilized, and Emp-solubilized cell fractions that were sequentially separated from M or G cells. The cytosolic fraction represents the soluble cellular fraction isolated after cell disruption in the absence of any detergent followed by high speed pelleting. The remaining postcytosolic pellet is then solubilized in NP-40 which, with regard to K8/18, would be expected to solubilize some of the membrane and "loosely associated" cytoskeletal fraction (Chou et al., 1994). The post–NP-40 pellet is then solubilized in Emp, which solubilizes a significant amount of the residual keratin fraction (Lowthert et al., 1995). As shown in Fig. 4 *A*, each cellular pool contains progressively increasing amounts of K8/18 after using equal fractions of each pool to immunoprecipitate K8/18 (compare lanes *1*, *3*, and *5* for G cells and lanes *2*, *4*, and *6* for M cells). In addition, there is a significant increase in the K8/18 cytosolic fraction of M cells as compared with G cells, as we observed previously when comparing G cells with colcemid-arrested G2/M cells (Chou et al., 1993). Differences in K8/18 content in the residual Emp fractions are not easily appreciated because of the limited amount of cytosolic K8/18 in G cells, which represents 5% of the total cellular keratin, and the overall large cellular keratin content (Chou et al., 1993).

To determine the stoichiometry of 14-3-3 and K8/18 association, K8/18 was isolated from each cellular fraction without normalizing the immunoprecipitation detergent conditions and with equal K8/18 loading per lane. As shown in Fig. 4 *B*, the keratin fractions that associated with 14-3-3 were cytosolic M > NP-40 M > cytosolic G.

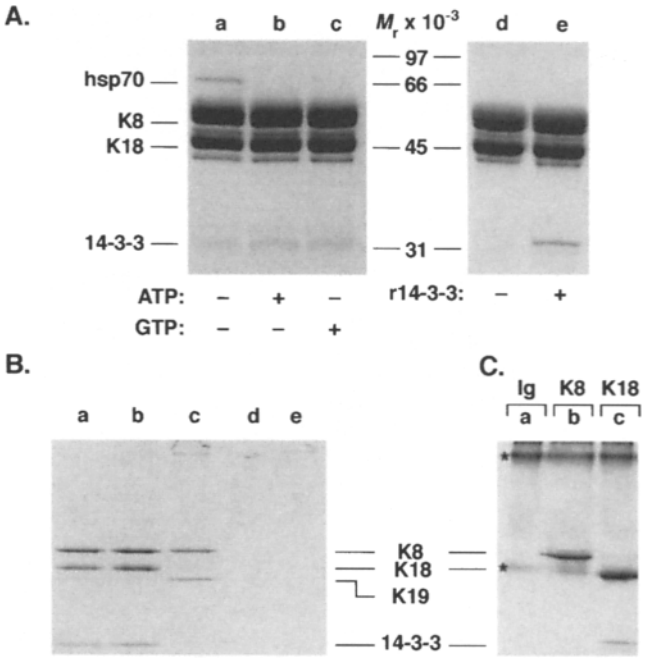

Figure 3. 14-3-3 binds to phospho-K18 and binding does not involve hsp70. (*A*) K8/18/19 immunoprecipitates were obtained from NP-40–solubilized OA-treated cells followed by treatment with $MgCl_2$/ATP or GTP (5 mM) that results in release of coimmunoprecipitated hsp70 but not 14-3-3 (lanes *a–c*). Alternatively, immunoprecipitates identical to those used in lane *b* (i.e., after hsp70 release) were incubated with 1% Emp in PBS to release the endogenous cellular 14-3-3 proteins (lane *d*), followed by incubation with r14-3-3 protein and then washing off unbound material (lane *e*). (*B*) An NP-40 lysate was obtained from M cells followed by incubation with mAb L2A1 which coimmunoprecipitates K8/18 with minimal K19 (lane *a*). The remaining L2A1-immunodepleted lysate was then incubated with mAb 4.62 to preferentially immunoprecipitate the residual K8/19 complexes (lane *c*). Alternatively, a sample of M cell NP-40 lysate equivalent to that used in lane *a* was first immunodepleted of K8/19 using mAb 4.62, followed by immunoprecipitation of the residual lysate with mAb CK5 to selectively isolate K8/18 without any K19 contamination (lane *b*). Control immunoprecipitates using mAb CK5 (lane *d*) and mAb 4.62 (lane *e*) without using a cell lysate are also shown. Immunoprecipitates were then incubated with 1% Emp in PBS to release bound cellular 14-3-3 proteins followed by incubation with r14-3-3. Of note, the endogenous 14-3-3 proteins that associated with the keratin immunoprecipitates showed an identical pattern to that obtained by binding of the r14-3-3 protein in lanes *a–c* (not shown). (*C*) K8 and K18 were individually purified from M cells as described in Materials and Methods, followed by incubation with r14-3-3 and then immunoprecipitation using rabbit antibody 8592 that recognizes K8 and K18. Background bands (*asterisks*) correspond to antibody (*Ig*). Lane *a* shows antibody incubated with r-14-3-3 and then isolated using protein A–Sepharose.

The keratin–14-3-3 association in the G cell cytosolic fraction occurs preferentially with a protein that comigrates with the ϵ isoform of 14-3-3 (Fig. 4 *B*, lane *1*). Since Emp treatment strips K8/18 of any bound 14-3-3, potential binding of 14-3-3 proteins to keratins from the Emp fraction was assessed and found not to occur after incubating Emp-stripped and washed K8/18 immunoprecipitates with Molt4 cytosol (Fig. 4 *C*, lanes *1* and *4*). Furthermore, 14-3-3 was not detected after analysis of the total protein content of the Emp fraction of HT29 G or M cells by immunoblotting, even though we estimate that ~0.2% of total HT29 cellular protein is 14-3-3ζ (not shown). Similar results to those shown in Fig. 4 *B* were also obtained if Emp-stripped K8/18 immunoprecipitates were incubated with r14-3-3 (not shown). Using r14-3-3 and purified K8/18 as standards, densitometric scanning of Coomassie-stained immunoprecipitates indicated that the stoichiometry of association is 0.5 molecule of 14-3-3 isoforms per molecule of cytosolic K18 in M cells, which represents ~6% of cytosolic 14-3-3ζ that is bound to cytosolic K8/18 at steady state in M cells (not shown).

Binding of 14-3-3 proteins to the cytosolic and NP-40–solubilized fractions of K8/18 (Fig. 4) and the importance of phosphorylation in facilitating this binding (Figs. 1 and 2) led us to examine K8/18 phosphorylation in the cytosolic, NP-40, Emp, and residual post-Emp fractions of G- and S-enriched cells. Metabolic labeling of G and S cells with $^{32}PO_4$ followed by analysis of the labeled K8/18 showed that cytosolic K8/18 had the highest $^{32}PO_4$ incorporation in G and S cells (Fig. 5 *A*). In addition to the increase in $^{32}PO_4$ incorporation in S cell K8/18, there is a significant shift in the ratio of the cytosolic K8/K18 labeling in G vs. S cells such that the ratio of K8 to K18 incorporated counts was 2.9 and 1.2, respectively (Fig. 5 *A*, lanes *1* and *4*; Table I). Most of the increase in incorporation in K8/18 labeling, when comparing S to G cell fractions, occured in the cytosolic and NP-40 fractions (Fig. 5 *A* and Table I), with the most significant increase being in the cytosolic fraction of K18 as compared with the increase in K8. To assess the overall state of K8/18 phosphorylation in the different fractions, we used isoelectric focusing/SDS-PAGE two-dimensional (2-D) analysis. As in Fig. 5 *A*, the majority of phosphorylated K8 and K18 isoforms are found in the cytosol of G cells (Fig. 5 *B*, *panel i*) and in the cytosol and NP-40 fraction of S cells (Fig. 5 *B*, *panels iv* and *v*). In fact, a significant percentage of K8/18 in these fractions is phosphorylated (Table I) as compared with the K8/18 Emp fractions from G and S cells that show low relative phosphorylation of K8 (isoforms *1* and *2*) and K18 (isoform *a*) and minimal labeling (Fig. 5 *B*, *panels iii* and *vi*). The 2-D pattern obtained from the K8/18 post-Emp pellet fraction was identical to the Emp K8/18 fraction for both G and S cells (not shown). Therefore, the distribution of phospho-K8/18 (Fig. 5 and Table I) parallels the cellular fractions that bind 14-3-3 (i.e., G cell cytosol, S/G2/M cell cytosol, and NP-40 fractions) (Fig. 4 *B*).

Since $^{32}PO_4$ labeling may interfere with normal progression through the cell cycle, we also analyzed the 2-D profile of K8/18 isolated from NP-40 fractions of G and S cells without labeling and without preseparation of the cytosolic fractions (Fig. 5 *C*). Under these isolation conditions, 14-3-3 binding to K8/18 from the G cell NP-40 fraction

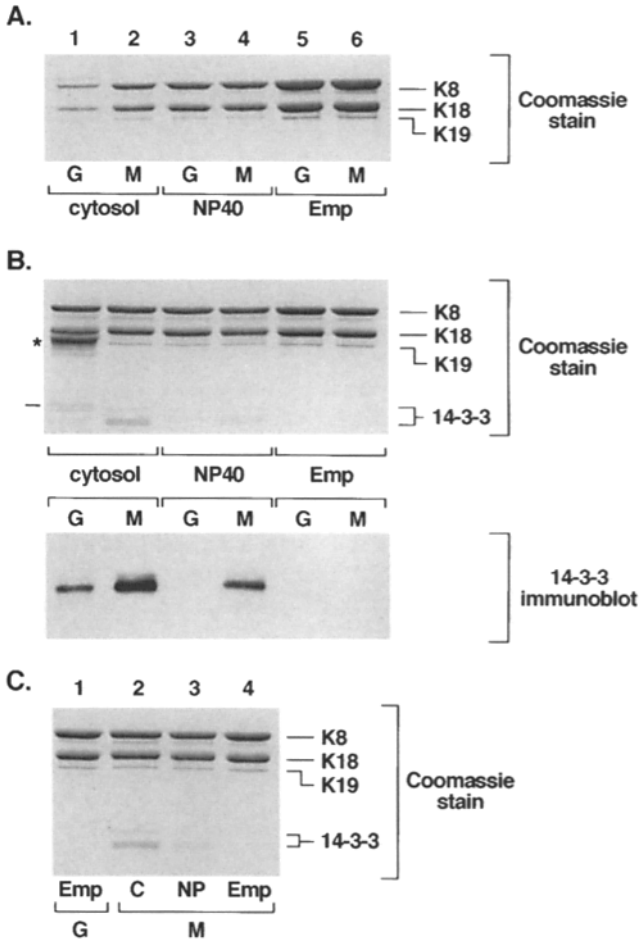

Figure 4. Characterization of 14-3-3 association with the cytosolic, NP-40–, and Emp-solubilized K8/18 fractions. (*A*) Equal numbers of G and M cells were disrupted by nitrogen cavitation followed by centrifugation to obtain the cytosolic fraction (C). The residual pellets were solubilized in 1% NP-40 in buffer A followed by centrifugation to obtain the supernatant NP-40 fraction. The post–NP-40 pellet was then solubilized in 1% Emp in buffer A followed by centrifugation and collection of the supernatant Emp fraction. Equivalent portions of each fraction were then used to immunoprecipitate K8/18 to show the relative keratin solubility in each of the three fractions. To normalize immunoprecipitation conditions, the solution composition of the isolated fractions was adjusted so that they all contained 1% NP-40 and 1% Emp. (*B*) K8/18 immunoprecipitates were obtained from the C, NP-40, and Emp fractions without adjustment of the detergent composition to maintain binding of endogenous 14-3-3 to K8/18. Nearly equal amounts of K8/18 were loaded per lane and analyzed by Coomassie staining or immunoblotting using anti–14-3-3ζ antibody. The identity of the K8/18-associated proteins (*small bar* and *asterisk* in lane *1*) are not conclusively known but may correspond to another 14-3-3 isoform and actin, respectively. (*C*) K8/18 immunoprecipitates identical to those used in *B* were incubated in 1% Emp/PBS to release the associated 14-3-3, followed by washing with PBS to remove residual Emp. Immunoprecipitates were then incubated with Molt4 lysate (30 min, 4°C), washed to remove unbound material, and analyzed by SDS-PAGE.

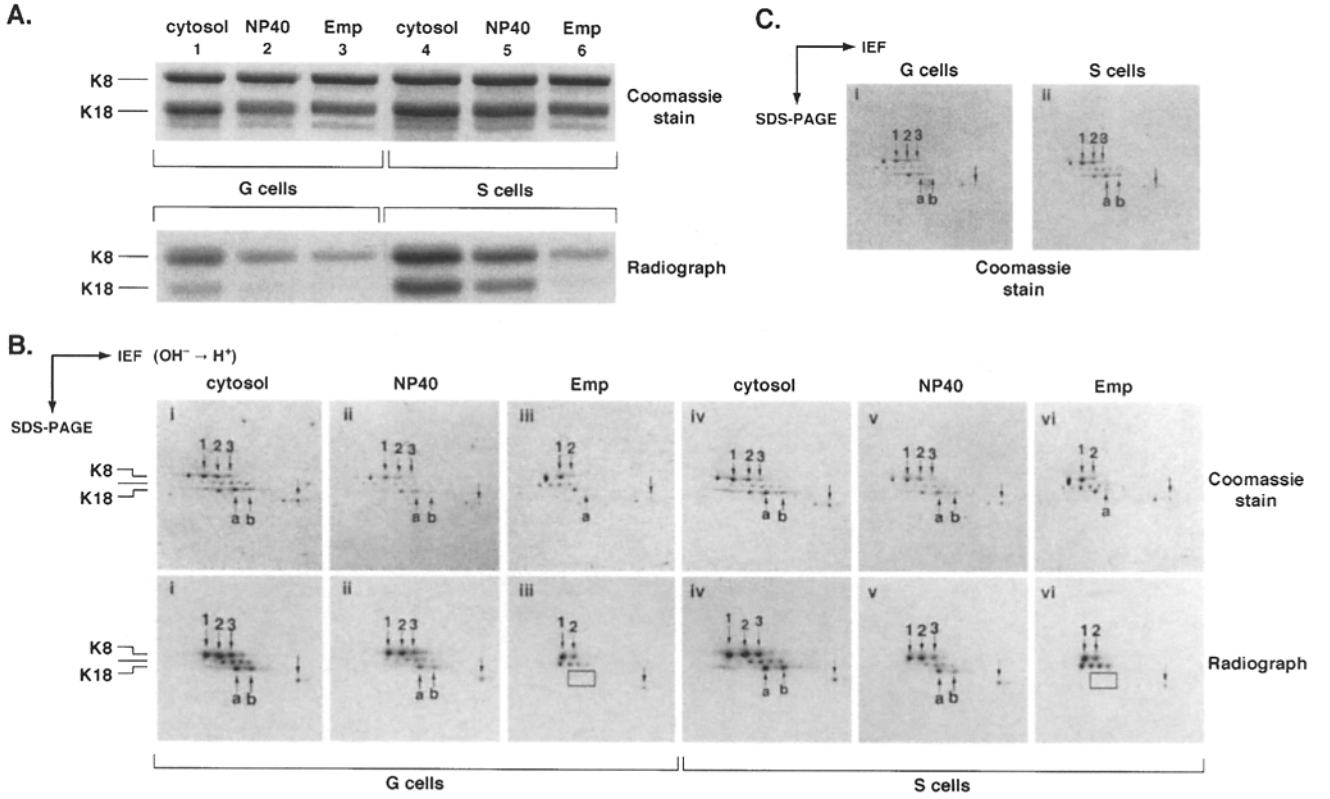

Figure 5. Phosphorylation gradient of K8/18 in cytosolic, NP-40, and Emp fractions. (*A*) HT29 near confluent cells (G cells) and S cells were labeled with $^{32}PO_4$ for 5 h followed by immunoprecipitation of K8/18 from sequentially isolated cytosolic, NP-40–solubilized, and Emp-solubilized fractions. Samples were normalized so that nearly equal K8/18 protein was loaded per lane. (*B*) Duplicate immunoprecipitates to those in *A* were analyzed in the horizontal direction by IEF followed by SDS-PAGE in the vertical direction. Arrows alone (K19), with numbers (*K8*), and with letters (*K18*), represent corresponding Coomassie-stained and $^{32}PO_4$-labeled isoforms. Boxes (radiograph profiles *iii* and *vi*) show the location where K18 isoforms would be seen on prolonged exposure (12 d; not shown). Exposure times of the radiographs were 72 (*ii*, *iii*, and *vi*), 48 (*i* and *v*), and 30 h (*iv*). Bar between K8 and K18 likely represents K20 or degraded K8. (*C*) Immunoprecipitates were obtained from an NP-40 lysate of nonlabeled G and S cells without initial removal of the cytosolic fraction followed by 2-D gel analysis. Major isoforms are indicated as in *B*.

cannot be appreciated, but K8/18 from the S cell NP-40 fraction binds to 14-3-3 (not shown but similar to Fig. 2). As shown in Fig. 5 *C*, the most dramatic acidic shift (consistent with increased phosphorylation) in isoforms occurs in K18 (isoforms *a* and *b*) and K19 (isoform indicated by *arrow*), whereas K8 isoforms 1–3 show a less prominent increase.

Effect of 14-3-3 on K8/18 Solubility In Vitro

Since 14-3-3 proteins preferentially bind to cytosolic K8/18, we asked if 14-3-3 can affect the in vitro solubility and assembly properties of K8/18. In doing so, we took advantage of the well-established ability of equal mixtures of urea-solubilized type I and type II keratins to self-assemble into 10-nm filaments after dialysis of the urea using low salt conditions (Quinlan et al., 1984). In the case of K8/18 purified from HT29 G cells and then assembled into filaments in vitro, most of the keratin is pelletable after a high speed spin with a barely detectable fraction that remains in solution (Liao et al., 1995*b*). This soluble fraction increases if the K8/18 used for assembly is obtained from heat-stressed HT29 cells that have hyperphosphorylated keratins (Liao et al., 1995*b*). Using this assay, we tested the ability of r14-3-3 protein to sequester K8/18 into the soluble fraction. The K8/18 was purified from NP-40–solubilized G or M cells or from an M cell Emp-solubilized post–NP-40 pellet (as an internal control for low K8/18 phosphorylation state). The soluble (i.e., nonpelletable) K8/18 fraction was then isolated, after assembly of K8/18 then incubation for 24 h in the absence or presence of 14-3-3 or soybean trypsin inhibitor. Soybean trypsin inhibitor was used as a control protein since it had a similar pI to 14-3-3 (Kunitz, 1947). As shown in Fig. 6 *A*, K8/18 solubility increased nearly threefold in keratins purified from NP-40–solubilized M cells as compared with keratins purified from NP-40–solubilized G cells (compare lanes *1* and *4*). This enhanced solubility in cytosolic M cell keratins increased further by more than twofold upon addition of 14-3-3 but was not affected by the addition of trypsin inhibitor (Fig. 6 *A*, lanes *4–6*). In contrast, the effect of 14-3-3 on the other two keratin fractions was minimal (Fig. 6 *A*, lanes *1–3* and *7–9*). The significant increase in solubility noted in K8/18 isolated from NP-40–solubilized M cells was commensurate with a significant decrease in the amount of residual K8/18 in the pellet as would be expected (Fig. 6 *A*, lane *5*). A similar 14-3-3–induced increase in K8/18 solubility was noted if 14-3-3 was added to

Table I. Quantitation of K8/18 Phosphorylation in Cytosolic, NP-40, and Emp Fractions

	G cells			S cells		
	Cytosol	NP-40	Emp	Cytosol	NP-40	Emp
$^{32}PO_4$ incorporation						
K8*	1.8	1.2	1*	3.8	2.4	1.3
K18‡	3.0	2.1	1‡	15.7	9.6	2.1
K8/18§	2.9	2.8	4.9	1.2	1.2	2.9
Percentage of phosphorylation‖						
K8	72%	28%	20%	72%	68%	36%
K18	54%	22%	8%	74%	65%	12%

The results shown in Fig. 5, *A* and *B* were quantitated. The cpm of $^{32}PO_4$ incorporated into K8 and 18 were determined by counting the corresponding bands from K8/18 immunoprecipitates shown in Fig. 5 *A*.

*Normalized phosphate incorporation was determined for K8 as:

$$\frac{\text{cpm for each K8 fraction (from G or S cells)}}{\text{cpm of K8 from G cell Emp fraction.}}$$

‡*Normalized phosphate incorporation for K18 was determined as:*

$$\frac{\text{cpm for each K18 fraction (from G or S cells)}}{\text{cpm of K18 from G cell Emp fraction.}}$$

§*The ratio of K8 to K18 $^{32}PO_4$ incorporation was determined for each fraction as:*

$$\frac{\text{cpm K8}}{\text{cpm K18.}}$$

‖The percentage of phosphorylation of K8 and K18 was individually determined by scanning the Coomassie-stained 2-D gels shown in Fig. 5 *B*. For each K8 or 18 fraction, % Phosphorylation = ([sum of densitometry units of numbered (K8) or lettered (K18) isoforms] ÷ [sum or densitometry units of all K8 or K18 isoforms]) × 100. This calculation makes the assumption that the isoforms (Fig. 5 *B*; 1–3 or *a* and *b*) are generated solely by phosphorylation and that the most basic isoforms (i.e., those not highlighted by numbered or lettered arrows) are not phosphorylated. The latter assumption is based on lack of in vivo phosphate labeling of the most basic isoforms.

the keratins before assembly (Fig. 6 *B*, lane *5*) with a consequent decrease in the amount of K8/18 in the pellet fraction (not shown) that was similar to that shown in Fig. 6 *A*. Both 14-3-3 and trypsin inhibitor remain in the soluble fraction and are not found in the pellet, whether added after (Fig. 6 *A*) or before assembly (Fig. 6 *B* and not shown). Of note, urea treatment of K8/18 (isolated from NP-40–solubilized M cells) and r14-3-3, followed by dialysis in low salt buffer, does not affect the competency of K8/18 to bind 14-3-3, and K8/18 complexed with 14-3-3 but not trypsin inhibitor can be coimmunoprecipitated using anti-K8/18 antibodies (not shown).

We then tested the effect of 14-3-3 on the in vitro filament-forming ability of K8/18 purified from NP-40–solubilized G or M cells or from the Emp-solubilized post–NP-40 pellet of M cells, with the latter fraction serving as an internal control. As shown in Fig. 7, 14-3-3 has a moderate effect on filament formation of keratins isolated from the NP-40 fraction of G cells or the Emp fraction of M cells, in that it results in looser and less extensive filament formation (compare *a* and *b* with *d* and *e*). In contrast, soybean trypsin inhibitor did not interfere with filament formation of keratins isolated from the Emp fraction (Fig. 7 *f*) or from the NP-40 fraction of G cells (not shown). We did not detect the typical filaments in the case of keratins purified from the NP-40 fraction of M cells (i.e, the fraction that has a high keratin phosphorylation state), although rare thin filaments were occasionally noted (Fig. 7 *c*, *small arrow*). Inclusion of 14-3-3 or trypsin inhibitor during the filament assembly assay of the NP-40 fraction of M cells had no discernible effect and resulted in a pattern (not shown) similar to that in Fig. 7 *c*.

Discussion

The major findings of this study are: (*a*) demonstration of a dynamic and phosphorylation-dependent association between 14-3-3 proteins and glandular keratins, specifically phospho-K18, during the S/G2/M phases of the cell cycle; (*b*) presence of a phosphorylation gradient in cells that correlates with keratin solubility and binding to 14-3-3 proteins; and (*c*) 14-3-3 enhancement of K8/18 solubility in vitro.

Association of 14-3-3 Proteins with Simple-type Epithelial Keratins

Phosphorylation of K8/18 appears to be the essential signal that facilitates association with 14-3-3. For example, hyperphosphorylation of K8/18 during the S/G2/M stages of the cell cycle (Fig. 2), or as a consequence of heat stress or okadaic acid treatment of cells (Fig. 1), results in coimmunoprecipitation of 14-3-3 proteins with K8/18. The association can be specifically reconstituted, after stripping off bound 14-3-3 using Emp, by the addition of r14-3-3 or cytosol from HT29 epithelial cells that have been depleted of K8/18 or cytosol from Molt4 lymphoid cells that do not express keratins (Fig. 1). Furthermore, the 14-3-3–keratin complex can be dissociated upon treatment with phosphatase, and its formation can be prevented if K8/18 is dephosphorylated (Fig. 2). The association of 14-3-3 with phospho-K8/18 reinforces the accumulating evidence that phosphorylation is important for ligand binding to 14-3-3 as demonstrated for Raf and Bcr (Michaud et al., 1995) and tryptophan hydroxylase (Furukawa et al., 1993). The molecular basis of this interaction remains to be investigated, but recent crystal structure analysis of the human T cell 14-3-3 τ isoform (Xiao et al., 1995) and 14-3-3 ζ isoform (Liu et al., 1995) provides some clues. These structural studies revealed that 14-3-3 proteins form a groove, with the outer lining consisting of varient amino acid residues and the inner lining consisting of highly conserved residues. The inner groove presents lysine and arginine residues that are typically invoked in phosphoamino acid binding.

Our results also point to the importance of K18 phosphorylation from quantitative and functional standpoints during cell cycle progression. For example, the relative increase in K18 phosphorylation is more pronounced than in that of K8 during S/G2/M phases of the cell cycle (Fig. 5), even though basal K18 phosphorylation is less than K8. This raises a question, which remains to be investigated, of whether other type I keratins manifest similar phosphorylation and 14-3-3 binding profiles. Support for the dramatic increase in K18 phosphorylation is based on in vitro labeling and 2-D gel analysis. Similarly, the high stoichiometry of phospho-K18 and 14-3-3 association is supported by finding that >50% of cytosolic and NP-40–associated S cell K18 is phosphorylated (Fig. 5 and Table I).

Potential Functional Significance of 14-3-3 Association with Keratins

The potential significance of 14-3-3 binding to K8/18 is

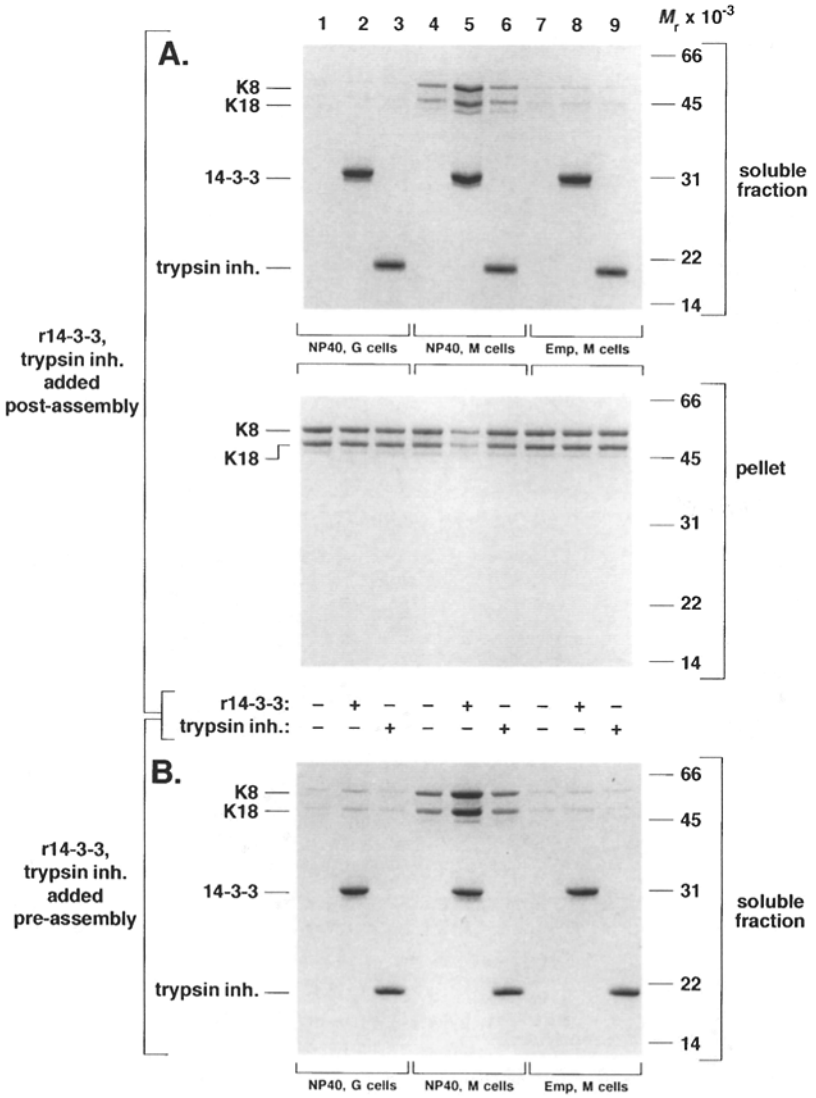

Figure 6. Effect of 14-3-3 on in vitro solubility of K8/18. K8/18 were purified by immunoprecipitation from HT29 G or M cells that were solubilized with NP-40 or from the Emp fraction of M cells that was obtained after removal of the NP-40 fraction. Immunoprecipitates were incubated in 1% Emp/PBS to release bound endogenous 14-3-3 proteins. Keratins were released from the covalently coupled antibody–agarose beads by incubation in 9.5 M urea, which results in release of only the keratins. (*A*) Immunopurified keratins (150 μg/ml) were dialyzed against 50 mM Tris-HCl/2 mM EDTA, pH 7.5 (36 h), followed by addition of buffer alone, 14-3-3, or trypsin inhibitor (62.5 μg/ml). After gentle rotation (24 h, 4°C), samples were pelleted (68,000 *g*, 30 min). Equivalent soluble and pellet fractions were then analyzed by SDS-PAGE. Some variability was noted in the recoverable pellet fraction due to variable adherence to the dialysis tubing but, regardless, the pellet sample corresponding to lane 5 was reproducibly the smallest (n = 3; not shown). (*B*) Purified keratins (150 μg/ml) were dialyzed as in *A* except that 14-3-3 or trypsin inhibitor (40 μg/ml) were added just before dialysis. After dialysis (36 h, 4°C) and pelleting, equivalent fractions of the soluble fraction were analyzed by SDS-PAGE. The pellet fractions had a pattern similar to that in *A* (not shown).

several-fold (Fig. 8). First, binding is stoichiometrically significant (~0.5 molecules of 14-3-3/keratin molecule). Since binding occurs preferentially with K18 (Fig.3), and given the tetrameric nature of simple epithelial keratins (Quinlan et al., 1984), including cytosolic K8/18 in HT29 cells (Chou et al., 1993), we estimate that each keratin tetramer (i.e., two K18 and two K8 molecules) binds to approximately one molecule of 14-3-3 in the cytosol of S/G2/M cells. This may be an underestimate since the percentage of S/G2/M cells in our synchronization experiments was ~60% (Fig. 2), with a range that sometimes peaks at ~90% (e.g., Liao et al., 1995*a*). Hence, a substantial fraction of the cytosolic and NP-40–solubilized K8/18 during S/G2/M is bound to 14-3-3. Furthermore, binding of K8/18 to 14-3-3 appears to be of high affinity, not affected by high salt (4 M NaCl) (not shown), ATP/GTP, or EDTA (Fig. 3), but it is abolished in the presence of zwitterionic detergents (e.g., Emp) or treatment with phosphatase (Fig. 2). Second, binding of 14-3-3 to K8/18 occurs in a regulated (i.e., phosphorylation-dependent) and reversible fashion during the cell cycle. Although the role of 14-3-3 proteins in higher eukaryotes is not known, yeast 14-3-3 homologs play an important role in determining the timing of mitosis in *Schizosaccharomyces pombe* (Ford et al., 1994). Given the association of 14-3-3 proteins with important cellular kinases such as PKC and Raf (for review see Aitken, 1995; Burbelo and Hall, 1995), PI3-kinase (Bonnefoy-Bérard et al., 1995), cdc25 phosphatases (Conklin et al., 1995), and with vesicular transport and Ras signaling (Gelperin et al., 1995), intracellular signaling or regulatory roles for 14-3-3 association with K8/18 become highly attractive. It remains to be determined if the observed association of PKC-related kinases with K8/18 (Omary et al., 1992) or with vimentin (Murti et al., 1992; Spudich et al., 1992) is based on direct or indirect association with 14-3-3, and if the K8/18 association with 14-3-3 modulates the activity of keratin and/or 14-3-3–associated kinases and phosphatases. Third, 14-3-3 proteins have been implicated in several other functions including priming of regulated exocytosis (Morgan and Burgoyne, 1992; Chamberlain et al., 1995) and activation of several enzymes including mono-ADP-ribosyltransferase (Fu et al., 1993) and tyrosine and tryptophan hydroxylases (Ichimura et al., 1988). It will be important to determine if binding of ker-

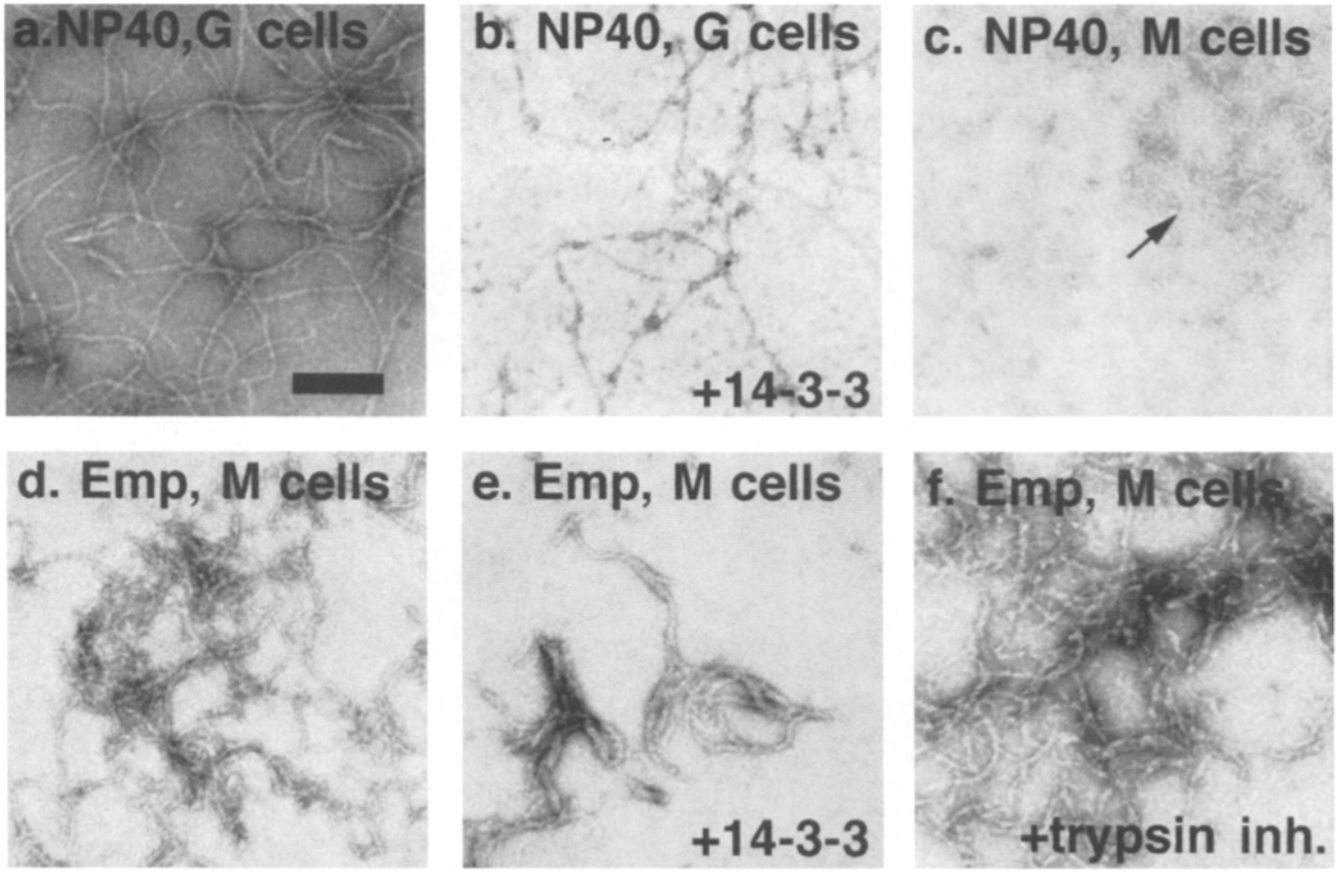

Figure 7. Effect of 14-3-3 on in vitro filament assembly of K8/18. Keratin in vitro filament assembly was carried out using samples identical to those used in Fig. 6 *B*. After dialysis, an aliquot was used for negative staining and then electron microscopy. All micrographs were obtained at the same magnification. Bar, 210 nm.

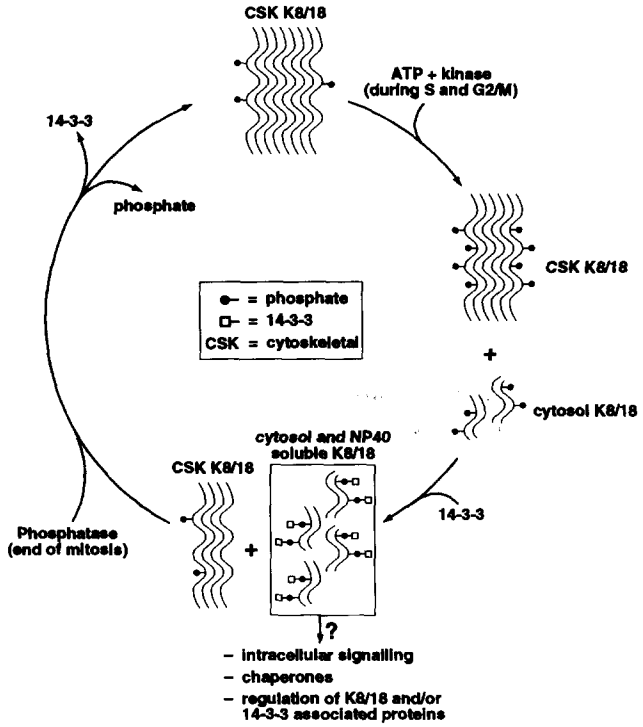

Figure 8. Proposed model for the dynamic K8/18 phosphorylation, binding to 14-3-3, and effect on solubility during the cell cycle. The cytoskeletal filamentous portion of K8/18, which makes up the major portion of K8/18 during the G1 phase of the cell cycle, becomes hyperphosphorylated during the S and G2/M phases of the cell cycle. Increased K8/18 phosphorylation increases the soluble K8/18 pool, followed by binding of 14-3-3 proteins to soluble K8/18 and sequestering of additional K8/18 into the soluble and NP-40 fractions. Dephosphorylation of keratins at the end of mitosis releases 14-3-3 and returns K8/18 into a G1 cytoskeletal state.

atins to 14-3-3 plays any role in altering the activity of keratin or 14-3-3–associated kinase or nonkinase enzyme activities, or if binding of 14-3-3 to soluble keratins simply displaces the enzymes that bind 14-3-3 or keratin to make them available in a "free" state that may be more or less active, depending on the nature of their 14-3-3– or keratin-bound states. Fourth, abundance of K8/18 (5% of HT29 total cell protein [Chou et al., 1993] with similar levels in several other epithelial cell lines tested [not shown]), and of 14-3-3 proteins (0.2% of HT29 total cell protein for the ζ isoform [this study] and 1% of total brain protein [Boston et al., 1982] raises the possibility of a chaperone-like role for the keratin–14-3-3 complex. To that end, 14-3-3 is the second abundant protein family to be shown to interact with K8/18, the first being the heat stress–induced and cognate hsp70 proteins (Liao et al., 1995*c*). In the case of hsp70, the interaction with keratins is ATP dependent and occurs preferentially with K8 (Liao et al., 1995*c*) but does

not interfere with K8/18 binding to 14-3-3 (Fig. 3). In addition, there is evidence for 14-3-3 proteins acting as mitochondrial import chaperones of cytoplasmic proteins in rat liver (Alam et al., 1994). Fifth, the potential of keratins to act as "linkers" or "soluble platforms" that can bring in close proximity different proteins may provide a mechanism that allows an interaction that otherwise may not occur at high efficiency. To that end, several findings including the presence of 14-3-3 proteins as homo- and heterodimers (Jones et al., 1995), recent evidence that 14-3-3 dimers may act as adaptors that can concurrently bind Raf and Bcr (Braselmann and McCormick, 1995), and the presence of a plekstrin homology domain (which is implicated in the functional interaction with a number of intracellular signal transduction proteins) (for review see Gibson et al., 1994) in 14-3-3 proteins including the ζ isoform (Dellambra et al., 1995) all support a putative linker or soluble platform role for keratin–14-3-3 interaction. Sixth, modulation of K8/18 solubility as described below.

Modulation of K8/18 Solubility by Phosphorylation and Binding to 14-3-3

We previously showed that ~5% of the keratin content of HT29 cells that are grown asynchronously (i.e., G0/G1 stage of the cell cycle) are soluble (Chou et al., 1993). Several studies in cultured cells uniformly showed a direct correlation between the level of K8/18 phosphorylation and their solubility. For example, the soluble K8/18 pool increases under conditions of mitotic arrest using antimicrotubule agents (Chou and Omary, 1993), the S/G2/M phases of the cell cycle (Fig. 4), heat stress (Liao et al., 1995*b*,*c*), and treatment of cells with phosphatase inhibitors such as okadaic acid and calyculin (not shown) with a parallel increase in K8/18 phosphorylation. In addition to these studies in cultured cells, there is direct in vitro evidence for phosphorylation playing an important role in K8/18 solubility after phosphorylation of purified K8/18 using any one of several kinases tested (Yano et al., 1991). Also, in vitro filament assembly of purified K8/18 from mitotically enriched cells (Fig. 6) or from heat-stressed cells (Liao et al., 1995*b*) (which contain high levels of phospho-K8/18) generates more soluble K8/18 than that obtained after assembly of K8/18 purified from G cells.

In addition to phosphorylation, our study also provides in vitro evidence for a 14-3-3 role as a K8/18 solubililty cofactor, which is unique from several aspects. For example, there is no known solubility protein cofactor for keratins, and the only other protein shown in vitro to act as an IF protein solubility cofactor is α-crystallin, which increases the solubility of vimentin and glial fibrillary acidic protein if added during in vitro filament assembly (Nicholl and Quinlan, 1994). Involvement of 14-3-3 as a K8/18 solubility cofactor occurs only under cell conditions when K8/18 phosphorylation increases such as during cell cycle progression. In the case of α-crystallin association with vimentin or glial fibrillary acidic protein, phosphorylation did not appear to play a role (Nicholl and Quinlan, 1994). The effect of 14-3-3 as a K8/18 solubility cofactor was specific since soybean trypsin inhibitor added under the same conditions had no effect (Fig. 6), and hsp70 binding to K8/18 also did not affect K8/18 solubility (Liao et al., 1995*c*). Both hsp70 and soybean trypsin inhibitor are acidic proteins with similar pIs to 14-3-3. Hence, the regulated interaction of 14-3-3 with cytosolic K8/18 and its potential solubilizing effect lend support to the hypothesis that either of these two abundant proteins may act as chaperones to one another or to other associated proteins (Fig. 8).

The observed in vitro effects of 14-3-3 on K8/18 filament assembly (Fig. 7) are unclear and remain to be investigated. For example, r14-3-3 ζ protein had a severing effect with resultant generation of less extended filaments in keratins isolated from NP-40–solubilized G cells or the Emp fraction of M cells. Such an effect is presumably based on limited binding to the minor population of phosphokeratins in these fractions. Several explanations can be envisioned, which remain to be tested, that may explain this observation. These include the presence, in vivo, of filament stabilizing proteins or that the observation is simply an in vitro phenomenon since no significant effect of 14-3-3 on keratin solubility was noted in these fractions (Fig. 6 *B*).

The phosphorylation gradient that we observed (Fig. 5) supports a role for keratin phosphorylation in its solubility and provides three potentially functional keratin compartments: cytosolic, NP-40 soluble, and Emp soluble. This gradient reflects a progressive decrease in the percentage of phosphorylated keratins within three compartments (Table I) that predominantly consist of cytosolic, membrane, and cytoskeletal domains. Analysis of the total M cell protein from these three compartments showed that 14-3-3 was present and associated with K8/18 only in the cytosolic and NP-40 compartments. Our previous analysis of keratins associated with various subcellular fractions (Chou et al., 1994) and the subcellular localization of 14-3-3 in rat brain (Martin et al., 1994) indicate that the NP-40 pool likely represents membrane-associated K8/18 and, potentially in addition, loosely associated cytoskeletal filamentous keratin. The Emp K8/18 pool, based on its sheer amount, likely represents the solubilized cytoskeletal fraction primarily, with a potential small amount of residual membrane- and/or other organelle-associated keratin. We did not observe this phosphorylation gradient in a previous study (Chou et al., 1993) for several reasons, including rapid K8/18 dephosphorylation in the cytosolic fraction if okadaic acid is not added immediately after cell disruption, duration of labeling with $^{32}PO_4$, and because 2-D gel analysis that provides overall assessment of keratin phosphorylation was not done in the earlier study. It remains to be determined if the phosphorylation gradient observed for K8/18 applies to other phosphokeratins or to other IF proteins.

In conclusion, the regulated and cell cycle–associated interaction of K8/18 with 14-3-3 proteins opens several exciting avenues for exploration. For example, potential roles for keratins as chaperones, linker, or soluble platform molecules, regulators of 14-3-3–associated proteins, and players in cell signaling can now be investigated.

We are very grateful to Linda P. Jacob and Romola L. Breckenridge for preparing the manuscript, Kris Morrow for preparing the figures, Lori A. Lowthert for assistance with some of the experiments, Dr. Young Moo Lee (University of California Davis, Protein Structure Laboratory) for performing the microsequencing, and Nafisa Ghori and Sarah Azad for assistance with the electron microscopy.

This work was supported by Veterans Administration Merit and Career

Development awards, a National Institutes of Health grant (DK47918), and a Digestive Disease Center grant (DK38707).

Received for publication 8 December 1995 and in revised form 3 February 1996.

References

Aitken, A. 1995. 14-3-3 proteins on the MAP. *Trends Biochem. Sci.* 20:95–97.

Alam, R, N. Hachiya, M. Sakaguchi, S. Kawabata, S. Iwanaga, M. Kitajima, K. Mihara, and T. Omura. 1994. cDNA cloning and characterization of mitochondrial import stimulation factor (MSF) purified from rat liver cytosol. *J. Biochem.* 116:416–425.

Baribault, H., R. Blouin, L. Bourgon, and N. Marceau. 1989. Epidermal growth factor–induced selective phosphorylation of cultured rat hepatocyte 55-kD cytokeratin before filament reorganization and DNA synthesis. *J. Cell Biol.* 109:1665–1676.

Bonnefoy-Bérard, N., Y.-C. Liu, M. von Willebrand, A. Sung, C. Elly, T. Mustelin, H. Yoshida, K. Ishizaka, and A. Altman. 1995. Inhibition of phosphatidylinositol 3-kinase activity by association with 14-3-3 proteins in T cells. *Proc. Natl. Acad. Sci. USA.* 92:10142–10146.

Boston, P.F., P. Jackson, and R.J. Thompson. 1982. Human 14-3-3 protein: radioimmunoassay, tissue distribution, and cerebrospinal fluid levels in patients with neurological disorders. *J. Neurochem.* 38:1475–1482.

Bowden, P.E., J.L. Haley, A. Kansky, J.A. Rothnagel, D.O. Jones, and R.J. Turner. 1995. Mutation of a type II keratin gene (K6a) in pachyonychia congenita. *Nat. Genet.* 10:363–365.

Boyle, W.J., P. Van Der Geer, and T. Hunter. 1991. Phosphopeptide mapping and phosphoamino acid analysis by two-dimensional separation on thin layer cellulose plates. *Methods Enzymol.* 201:110–149.

Braselmann, S., and F. McCormick. 1995. BCR and RAF form a complex *in vivo* via 14-3-3 proteins. *EMBO (Eur. Mol. Biol. Organ.) J.* 14:4839–4848.

Burbelo, P.D., and A. Hall. 1995. Hot numbers in signal transduction. *Curr. Opin. Cell Biol.* 5:95–96.

Busso, N., S.K. Masur, D. Lazega, S. Waxman, and L. Ossowski. 1994. Induction of cell migration by pro-urokinase binding to its receptor: possible mechanism for signal transduction in human epithelial cells. *J. Cell Biol.* 126: 259–270.

Calnek, D., and A. Quaroni. 1993. Differential localization by in situ hybridization of distinct keratin mRNA species during intestinal epithelial cell development and differentiation. *Differentiation.* 53:95–104.

Celis, J.E., P.M. Larsen, S.J. Fey, and A. Celis. 1983. Phosphorylation of keratin and vimentin polypeptides in normal and transformed mitotic human epithelial amnion cells: behavior of keratin and vimentin filaments during mitosis. *J. Cell Biol.* 97:1429–1434.

Chamberlain, L.H., D. Roth, A. Morgan, and R.D. Burgoyne. 1995. Distinct effects of α-SNAP, 14-3-3 proteins, and calmodulin on priming and triggering of regulated exocytosis. *J. Cell. Biol.* 130:1063–1070.

Chou, C.-F., and M.B. Omary. 1993. Mitotic-arrest associated enhancement of O-linked glycosylation and phosphorylation of human keratins 8 and 18. *J. Biol. Chem.* 268:4465–4472.

Chou, C.-F., and M.B. Omary. 1994. Mitotic arrest with anti-microtubule agents or okadaic acid is associated with increased glycoprotein terminal GlcNAc's. *J. Cell Sci.* 107:1833–1843.

Chou, C.-F., C.L. Riopel, L.S. Rott, and M.B. Omary. 1993. A significant soluble keratin fraction in "simple" epithelial cells: lack of an apparent phosphorylation and glycosylation role in keratin solubility. *J. Cell Sci.* 105:433–445.

Chou, C.-F., C.L. Riopel, and M.B. Omary. 1994. Identification of a keratin-associated protein that localizes to a membrane compartment. *Biochem. J.* 298:457–463.

Conklin, D.S., K. Galaktionov, and D. Beach. 1995. 14-3-3 proteins associate with cdc25 phosphatases. *Proc. Natl. Acad. Sci. USA.* 92:7892–7896.

Dellambra, E., M. Patrone, B. Sparatore, A. Negri, F. Ceciliani, S. Bondanza, F. Molina, F.D. Cancedda, and M. De Luca. 1995. Stratifin, a keratinocyte specific 14-3-3 protein, harbors a pleckstrin homology (PH) domain and enhances protein kinase C activity. *J. Cell Sci.* 108:3569–3579.

Eckert, R.L. 1988. Sequence of the human 40-kDa keratin reveals an unusual structure with very high sequence identity to the corresponding bovine keratin. *Proc. Natl. Acad. Sci. USA.* 85:1114–1118.

Evans, R.M. 1994. Intermediate filaments and lipoprotein cholesterol. *Trends Cell Biol.* 4:149–151.

Figlewicz, D.A., A. Krizus, M.G. Martinoli, V. Meininger, M. Dib, G.A. Rouleaue, and J.-P. Julien. 1994. Variants of the heavy neurofilament subunit are associated with the development of amyotrophic lateral sclerosis. *Human Mol. Genet.* 3:1757–1761.

Ford, J.C., F. Al-Khodairy, E. Fotou, K.S. Sheldrick, D.J.F. Griffiths, and A.M. Carr. 1994. 14-3-3 protein homologs required for the DNA damage checkpoint in fission yeast. *Science (Wash. DC).* 265:533–535.

Freed, E., M. Symons, S.G. Macdonald, F. McCormick, and R. Ruggieri. 1994. Binding of 14-3-3 proteins to the protein kinase Raf and effects on its activation. *Science (Wash. DC).* 265:1713–1716.

Fu, H., J. Coburn, and R.J. Collier. 1993. The eukaryotic host factor that activates exoenzyme S of *Pseudomonas aeruginosa* is a member of the 14-3-3 protein family. *Proc. Natl. Acad. Sci. USA.* 90:2320–2324.

Fu, H., K. Xia, D.C. Pallas, C. Cui, K. Conroy, R.P. Narsimhan, H. Mamon, R.J. Collier, and T.M. Roberts. 1994. Interaction of the protein kinase Raf-1 with 14-3-3 proteins. *Science (Wash. DC).* 266:126–129.

Fuchs, E., and K. Weber. 1994. Intermediate filaments: structure, dynamics, function and disease. *Annu. Rev. Biochem.* 63:345–382.

Fuchs, E., Y.-M. Chan, A.S. Paller, and Q.-C. Yu. 1994. Cracks in the foundation: keratin filaments and genetic disease. *Trends Cell Biol.* 4:321–326.

Furukawa, Y., N. Ikuta, S. Omata, T. Yamauchi, T. Isobe, and T. Ichimura. 1993. Demonstration of the phosphorylation-dependent interaction of tryptophan hydroxylase with the 14-3-3 protein. *Biochem. Biophys. Res. Commun.* 194:144–149.

Gelperin, D., J. Weigle, K. Nelson, P. Roseboom, K. Irie, K. Matsumoto, and S. Lemmon. 1995. 14-3-3 proteins: potential roles in vesicular transport and Ras signaling in *Saccharomyces cerevisiae. Proc. Natl. Acad. Sci. USA.* 92: 11539–11543.

Gibson, T.J., M. Hyvönen, A. Musacchio, and M. Saraste. 1994. PH domain: the first anniversary. *Trends Biochem. Sci.* 19:349–353.

Ichimura, T., T. Isobe, T. Okuyama, N. Takahashi, K. Araki, R. Kuwano, and Y. Takahashi. 1988. Molecular cloning of cDNA for brain-specific 14-3-3 protein, a protein kinase-dependent activator of tyrosine and tryptophan hydroxylases. *Proc. Natl. Acad. Sci. USA.* 85:7084–7088.

Ichimura-Ohshima, Y., K. Morii, T. Ichimura, K. Araki, Y. Takahashi, T. Isobe, S. Minoshima, R. Fukuyama, N. Shimizu, and R. Kuwano. 1992. cDNA cloning and chromosome assignment of the gene for human brain 14-3-3 protein η chain. *J. Neurosci. Res.* 31:600–605.

Irie, K., Y. Gotoh, B.M. Yashar, B. Errede, E. Nishida, and K. Matsumoto. 1994. Stimulatory effects of yeast and mammalian 14-3-3 proteins on the Raf protein kinase. *Science (Wash. DC).* 265:1716–1719.

Jones, D.H., S. Ley, and A. Aitken. 1995. Isoforms of 14-3-3 protein can form homo- and heterodimers in vivo and in vitro: implications for function as adapter proteins. *FEBS Lett.* 368:55–58.

Klymkowsky, M.W., J.B. Bachant, and A. Domingo. 1989. Functions of intermediate filaments. *Cell Motil. Cytoskeleton.* 14:309–331.

Ku, N.-O., S. Michie, R.G. Oshima, and M.B. Omary. 1995. Chronic hepatitis, hepatocyte fragility, and increased soluble phosphoglycokeratins in transgenic mice expressing a keratin 18 conserved arginine mutant. *J. Cell Biol.* 131:1303–1314.

Ku, N.-O., and M.B. Omary. 1994. Identification of the major physiologic phosphorylation site of human keratin 18: potential kinases and a role in filament reorganization. *J. Cell Biol.* 127:161–171.

Kunitz, M. 1947. Crystalline soybean trypsin inhibitor. *J. Gen. Physiol.* 30:291–310.

Laemmli, U.K. 1970. Cleavage of structural proteins during the assembly of the head of bacteriophage T4. *Nature (Lond.).* 227:680–685.

Liao, J., L.A. Lowthert, N-O. Ku, R. Fernandez, and M.B. Omary. 1995*a*. Dynamics of human keratin 18 phosphorylation: Polarized distribution of phosphorylated keratins in simple epithelial tissues. *J. Cell Biol.* 131:1291–1301.

Liao, J., L.A. Lowther, and M.B. Omary. 1995*b*. Heat stress or rotavirus infection of human epithelial cells generates a distinct hyperphosphorylated form of keratin 8. *Exp. Cell Res.* 219:348–357.

Liao, J., L.A. Lowthert, N. Ghori, and M.B. Omary. 1995*c*. The 70-kDa heat shock proteins associate with glandular intermediate filaments in an ATP-dependent manner. *J. Biol. Chem.* 270:915–922.

Liu, D., J. Bienkowska, C. Petosa, R.J. Collier, H. Fu, and R. Liddington. 1995. Crystal structure of the zeta isoform of the 14-3-3 protein. *Nature (Lond.).* 376:191–194.

Lowthert, L.A., N-O. Ku, J. Liao, P.A. Coulombe, and M.B. Omary. 1995. Empigen BB: a useful detergent for solubilization and biochemical analysis of keratins. *Biochem. Biophys. Res. Commun.* 206:370–379.

Martín, H., J. Rostas, Y. Patel, and A. Aitken. 1994. Subcellular localisation of 14-3-3 isoforms in rat brain using specific antibodies. *J. Neurochem.* 63:2259–2265.

McLean, W.H.I., and E.B. Lane. 1995. Intermediate filaments in disease. *Curr. Opin. Cell Biol.* 7:118–125.

McLean, W.H.I., E.L. Rugg, D.P. Lunny, S.M. Morley, E.B. Lane, O. Swensson, P.J.C. Dopping-Hepenstal, W.A.D. Griffiths, R.A.J. Eady, C. Higgins et al. 1995. Keratin 16 and keratin 17 mutations cause pachyonychia congenita. *Nat. Genet.* 9:273–278.

Michaud, N.R., J.R. Fabian, K.D. Mathes, and D.K. Morrison. 1995. 14-3-3 is not essential for Raf-1 function: identification of Raf-1 proteins that are biologically activated in a 14-3-3- and Ras-independent manner. *Mol. Cell. Biol.* 15:3390–3397.

Moll, R., W.W. Franke, D.L. Schiller, B. Geiger, and R. Krepler. 1982. The catalog of human cytokeratins: patterns of expression in normal epithelia, tumors and cultured cells. *Cell.* 31:11–24.

Moll, R., D.L. Schiller, and W.W. Franke. 1990. Identification of protein IT of the intestinal cytoskeleton as a novel type I cytokeratin with unusual properties and expression patterns. *J. Cell Biol.* 111:567–580.

Moll, R., R. Zimbelmann, M.D. Goldschmidt, M. Keith, J. Laufer, M. Kasper, P.J. Koch, and W.W. Franke. 1993. The human gene encoding cytokeratin 20 and its expression during fetal development and in gastrointestinal carcinomas. *Differentiation.* 53:75–93.

Moore, B.W., and V.J. Perez. 1967. Specific acidic proteins of the nervous system. *In* Physiological and Biochemical Aspects of Nervous Integration (F.D. Carlson, editor). 343–359. Prentice-Hall, Englewood Cliffs, NJ.

Morgan, A., and R.D. Burgoyne. 1992. Exo1 and Exo2 proteins stimulate calcium-dependent exocytosis in permeabilized adrenal chromaffin cells. *Nature (Lond.)*. 355:833–836.

Murti, K.G., K. Kaur, and R.M. Goorha. 1992. Protein kinase C associates with intermediate filaments and stress fibers. *Exp. Cell Res.* 202:36–44.

Nicholl, I.D., and R.A. Quinlan. 1994. Chaperone activity of α-crystallins modulates intermediate filament assembly. *EMBO (Eur. Mol. Biol. Organ.) J.* 13:945–953.

Omary, M.B., G.T. Baxter, C-F. Chou, C.L. Riopel, W.Y. Lin, and B. Strulovici. 1992. PKCε-related kinase associates with and phosphorylates cytokeratin 8 and 18. *J. Cell Biol.* 117:583–593.

Oshima, R.G. 1982. Developmental expression of murine extra-embryonic endodermal cytoskeletal proteins. *J. Biol. Chem.* 257:3414–3421.

Quinlan, R.A., J.A. Cohlberg, D.L. Schiller, M. Hatzfeld, and W.W. Franke. 1984. Heterotypic tetramer (A_2D_2) complexes of non-epidermal keratins isolated from cytoskeletons of rat hepatocytes and hepatoma cells. *J. Mol. Biol.* 178:365–388.

Reuther, G.W., H. Fu, L.D. Cripe, R.J. Collier, and A.M. Pendergast. 1994. Association of the protein kinases c-Bcr and Bcr-Abl with proteins of the 14-3-3 family. *Science (Wash. DC)*. 266:129–133.

Richard, G., V. De Laurenzi, B. Didona, S.J. Bale, and J.G. Compton. 1995. Keratin 13 point mutation underlies the hereditary mucosal epithelia disorder white sponge nevus. *Nat. Genet.* 11:453–455.

Robinson, K., D. Jones, Y. Patel, H. Martin, J. Madrazo, S. Martin, S. Howell, M. Elmore, M.J. Finnen, and A. Aitken. 1994. Mechanism of inhibition of protein kinase C by 14-3-3 isoforms. *Biochem. J.* 299:853–861.

Roseboom, P.H., J.L. Weller, T. Babila, A. Aitken, L.A. Sellers, J.R. Moffett, M.A.A. Namboodiri, and D.C. Klein. 1994. Cloning and characterization of the ε and ζ isoforms of the 14-3-3 proteins. *DNA and Cell Biol.* 13:629–640.

Rugg, E.L., W.H.I. McLean, W.E. Allison, D.P. Lunny, R.I. Macleod, D.J. Felix, E.B. Lane, and C.S. Munro. 1995. A mutation in the mucosal keratin K4 is associated with oral white sponge nevus. *Nat. Genet.* 11:450–452.

Skalli, O., and R.D. Goldman. 1991. Recent insights into the assembly, dynamics, and function of intermediate filament networks. *Cell Motil. Cytoskeleton.* 19:67–79.

Spudich, A., T. Meyer, and L. Stryer. 1992. Association of the β isoform of protein kinase C with vimentin filaments. *Cell Motil. Cytoskeleton.* 22:250–256.

Stasiak, P.C., P.E. Purkis, I.M. Leigh, and E.B. Lane. 1989. Keratin 19: predicted amino acid sequence and broad tissue distribution suggest it evolved from keratinocyte keratins. *J. Invest. Dermatol.* 92:707–716.

Steinert, P.M., and D.R. Roop. 1988. Molecular and cellular biology of intermediate filaments. *Annu. Rev. Biochem.* 57:593–625.

Traub, P., and R.L. Shoeman. 1994. Intermediate filament and related proteins: potential activators of nucleosomes during transcription initiation and elongation? *Bioessays.* 16:349–355.

Yano, T., T. Tokui, Y. Nishi, K. Nishizawa, M. Shibata, K. Kikuchi, S. Tsuiki, T. Yamauchi, and M. Inagaki. 1991. Phosphorylation of keratin intermediate filaments by protein kinase C, by calmodulin-dependent protein kinase and by cAMP-dependent protein kinase. *Eur. J. Biochem.* 197:281–290.

Xiao, B., S.J. Smerdon, D.H. Jones, G.G. Dodson, Y. Soneji, A.A. Aitken, and S.J. Gamblin. 1995. Structure of a 14-3-3 protein and implications for coordination of multiple signalling pathways. *Nature (Lond.)*. 376:188–191.